

# Numerical modeling on brittle failure of coal wall in longwall face—a case study

Qing-Sheng Bai · Shi-Hao Tu · Xiao-Gang Zhang ·  
Cun Zhang · Yong Yuan

Received: 30 July 2013 / Accepted: 4 November 2013 / Published online: 21 November 2013  
© Saudi Society for Geosciences 2013

**Abstract** In China, as the shearer cutting height increases in longwall face, serious coal wall failure and spallings occur often, especially for brittle coal seam, which leads to large block spallings, equipment damage, and casualties. In this paper, 2D finite difference models are constructed, aiming to exam the brittle failure of coal wall during longwall mining in Majjaliang coal mine, Shuozhou, China. The strain-softening constitutive model is used to reveal the brittle failure characteristics of the coal wall. A numerical algorithm is developed to simulate the longwall goaf compaction process, and obtain the proper mining-induced stress around the longwall face. Based on extensive field surveys, three numerical models, i.e., intact coal wall, coal wall including vertical discontinuities and criss-cross discontinuities, are presented for investigating the brittle failure mode and spalling mechanism of the coal wall. The numerical results show that both coal wall failure modes and the failure (spalling) depths are in good agreement with the field observations. The simulations reveal that the sizes of the spalling blocks are closely related to the failure mode. For intact coal wall or coal wall including large space vertical discontinuities, occurrences of the large block spallings are favorable. For coal wall including small space vertical discontinuities and criss-cross discontinuities, small segment spallings play a dominant role. In light of this, analyses are conducted to investigate the effects of the face stoppage time and face guard on the failure mode and spallings of the coal wall. The result of this study indicates that the mining operation should accelerate and the length and pressure of the face guard should increase in this longwall face.

**Keywords** Numerical modeling · Brittle failure of coal wall · Longwall mining · Field observations · Goaf compaction process

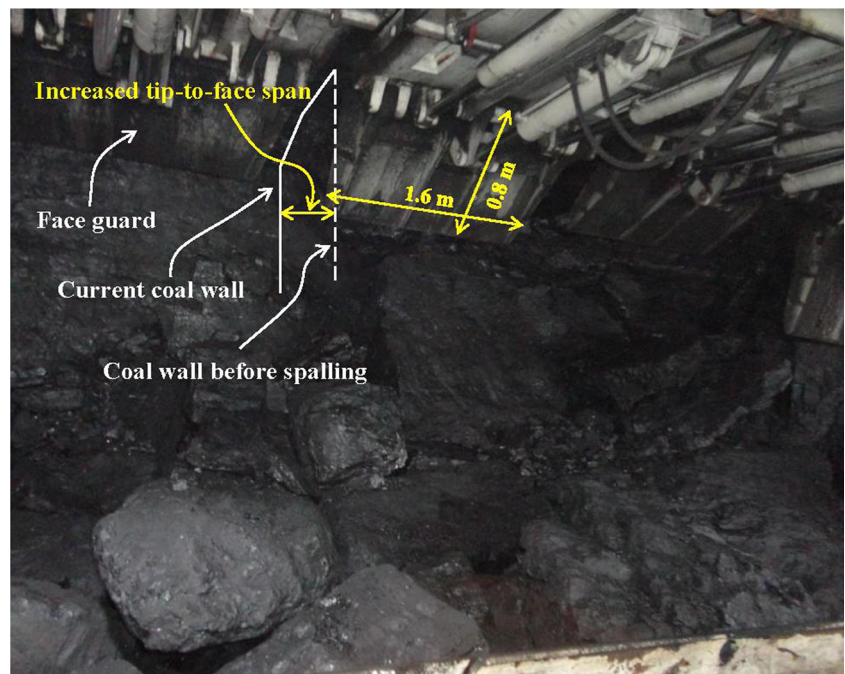
## Introduction

In China, with the development of mining equipment, the extraction height by shearer has increased to be 7.0 m in fully mechanized longwall face (Ju and Xu 2013). However, because of the great extraction heights and intense pressure around the longwall face induced by mining, serious coal wall spallings (defined as the skin failure and fall of the coal wall in longwall face as shown in Fig. 1) often occur. Serious coal wall spallings have been recognized as one of the major difficulties that affect the safety of the longwall face (Yuan et al. 2011; Ning 2009). Coal wall spallings enlarge the tip-to-face span (Fig. 1), hence, tend to cause roof falls (Ning 2009; Liu et al. 2008; Wang 2007). The coal wall spallings disturb the mining process. For severe cases, equipment damage and even casualties may occur. For example, in America, approximately 8 % of groundfall deaths are associated with skin fall of roof and face in longwall face (Pappas et al. 2000). Numerous efforts have been made to study the coal wall spallings induced by excavating soft coal seam (e.g., Zhu 2010; Wang 2007; Yuan et al. 2012; Liu et al. 2008), but examining mining brittle coal seams is rare in literature.

In general, soft coal causes small spallings, while brittle coal seam tends to form block spallings, as exhibited in Fig. 1. Taking the 14101 longwall face in Majjaliang coal mine for example, since the procreative seam is brittle, spallings with large size happen frequently, and the dimension of most of the blocks is  $5.2 \times 3.4 \times 0.7$  m (length  $\times$  height  $\times$  thickness). The block spallings cannot fully enter the chain conveyor, resulting in cumulation in the shearer corridor. The resistance produced by cumulated spallings is too high to move the chain

Q.-S. Bai · S.-H. Tu (✉) · X.-G. Zhang · C. Zhang · Y. Yuan  
Key Laboratory of Deep Coal Resource, Ministry of Education of  
China, School of Mines, China University of Mining and  
Technology, Xuzhou 221116, Jiangsu, China  
e-mail: papertsh@126.com

**Fig. 1** Brittle coal wall spillings in 14101 longwall face



conveyor, blocking the shearer corridor. The block spillings also jam the tail of the chain conveyor, and are too big to be conveyed into the reversed loader. Therefore, mining operation must be stopped to crush the block spillings and dredge the chain conveyor. Furthermore, when the coal wall contains

weak plane-like joints and beddings, the fractured coal wall tends to fall suddenly, which may cause casualties (Liu and Zhang 2010).

The impact of coal wall spalling is of great importance in mining operation. The serious coal wall spillings not only

**Fig. 2** A generalized stratigraphic column in 14101 longwall face (modified after (Bai et al. 2013))

No.	Thickness (m)	Depth(m)	Formation	Lithology	No.	Thickness (m)	Depth (m)	Formation	Lithology
1	224	224	soil		6	10	559	Siltstone	
2	126	350	Majority are mudstone and sand mudstone		7	5	564	Mudstone and kaoline	
3	114	464	Majority are fine and medium sandstone		8	5	569	Packstone	
4	70	534	Siltstone and packstone		9	5	574	Mudstone	
5	15	549	Majority are mudstone		10	9.1	583.1	#4 coal	
					11	2.5	585.6	Packstone	
					12	2.5	588.1	Siltstone	
					13	5	593.1	Sand mudstone	
					14	10	603.1	Siltstone	
					15	16.5	619.6	Sandstone & mudstone	
					16	8.6	628.2	Packstone	
					17	12.3	640.5	Sand mudstone	

cause mining to be discontinued, resulting in unnecessary economic losses, but also threaten the safety of workmen and equipment in the mining face. This paper used a two-dimensional finite difference method to simulate the brittle failure of coal wall in 14101 longwall face in Majialiang coal mine. The focus of this work is to study the failure mode of the coal wall with different types. In addition, the effects of face stoppage time and face guard (see Fig. 1) on the failure mode of the coal wall are also investigated.

**The study area**

Majialiang coal mine is located in the south of Shuozhou, Shanxi province, China. Panel 14101 is the first longwall face in the coal mine. The thickness of #4 seam in the panel is 6–11.0 m, with an average value of 9.1 m. A fully mechanized top-coal caving longwall face is set up to extract the #4 seam. In the face, a 3.5 m high longwall face is operated at the floor of the coal seam, and top-slice coal with a thickness of 2.5–7.5 m is caved and produced through the windows behind shields. The average depth below surface of #4 seam is 574 m. A generalized stratigraphic column showing the coal seam together with roof and floor strata is presented in Fig. 2.

**Numerical analysis on coal wall failure in longwall face**

Numerical simulation using finite difference model has become a powerful means in the design process of underground excavation and support, as well as in the investigation of physical mechanisms and failure mechanisms. To simulate and predict coal wall spalling more realistically, the mechanics response of the coal wall and stress distribution around the longwall face should be determined accurately, and appropriate numerical models are also needed. A detailed field survey was conducted to collect all the pertinent geological structures in the longwall face. According to geological condition in the mining area, three different coal wall types are considered in this study, as shown in Fig. 3. Type I is an intact coal wall model (see Fig. 3a), which examines the failure mode of the homogeneous coal wall without any discontinuities in the longwall face. Type II (see Fig. 3b) analyses the failure mode of the coal wall with a space of 0.15 m vertical discontinuities. Finally, for type III (see Fig. 3c), the effect of the criss-cross discontinuities on the failure mode of the coal wall is examined. The spaces of the vertical and horizontal discontinuities are 0.15 and 0.5 m, respectively. The strength parameters of the discontinuities are specified to 10 % of the coal seam (Esterhuizen et al. 2010).

The explicit finite difference model program FLAC2D is used in this study to setup numerical models to investigate the brittle failure of the coal wall concerning intact and

discontinuities coal wall as represented above. This detailed study includes approaches to simulate brittle failure, model setup, longwall goaf simulation, and comparison between numerical results and field observations.

**Approaches to simulate brittle failure**

Based on the complete strain–stress curve of a rock sample, the postfailure behavior of geomaterials can be classified into two types: ideal elastoplastic and strain-softening/hardening.

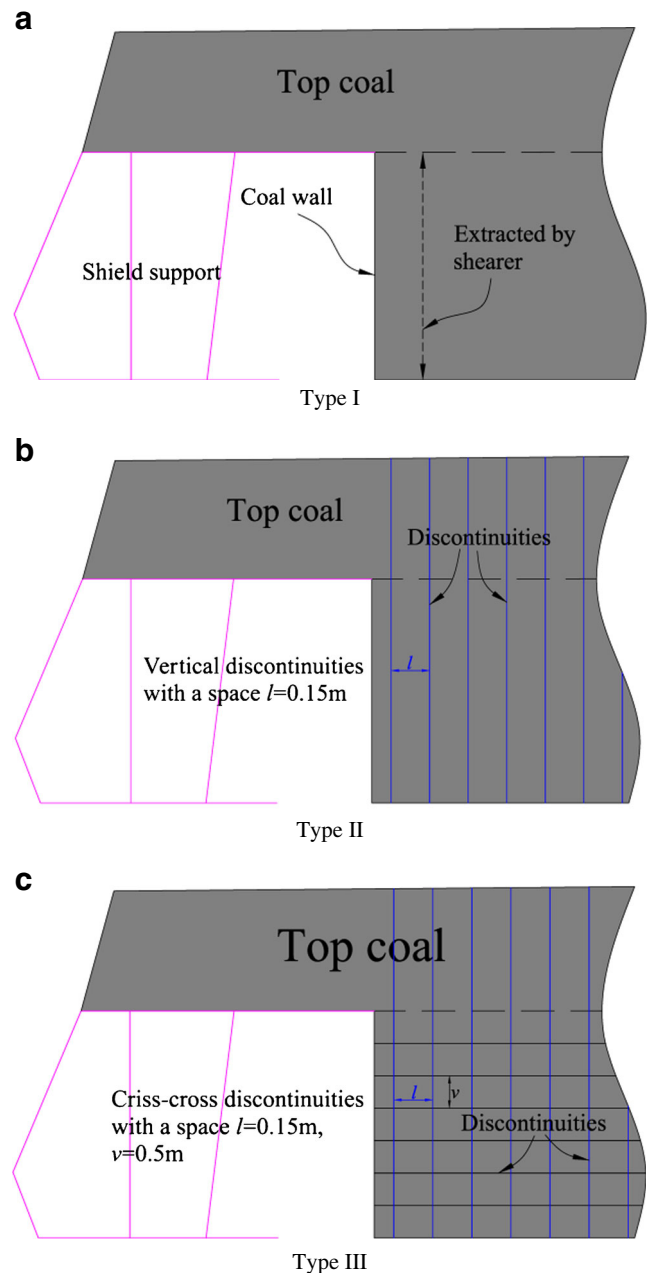


**Fig. 3** Numerical model setups (not in scales); **a** type I, intact coal wall; **b** type II, coal wall including vertical discontinuities; **c** type II, coal wall including criss-cross discontinuities

As we know, the elastoplastic and elastobrittle plastic models are just two typical and special types of strain-softening behavior (Zhang et al. 2012; Wang et al. 2011a, b). Strain-softening model has been widely used to model brittle failure in underground excavation (Wang et al. 2011a, b; Mortazavi et al. 2009; Edelbro 2010; Zhou et al. 2009; Schullera and Schweiger 2002; Bai et al. 2012).

In this study, the strain-softening model was used to simulate the uniaxial compression test, and the results are compared with the experimental data. The specimen of #4 coal fails in typical X-shaped brittle failure, as shown in Fig. 4a, b. The specimen strength plummets after the peak strength as shown in Fig. 4c. Clearly, numerical simulation results of both

the failure pattern and the stress–strain characteristics are in good agreement with that of experimental data. In the following simulations, strain-softening model is used to analyze the brittle failure of coal wall in the longwall face.

#### Model setup

The geometry and boundary conditions in this finite difference model are shown in Fig. 5. The length of the model is 600 m, including 320 m longwall goaf, longwall face of 8 m width, and the unmined region of 272 m in front of the longwall face. The height of the model is 212.1 m, including 144.9 m rock strata in the roof, 58.1 m rock strata in the floor, and #4 coal seam of

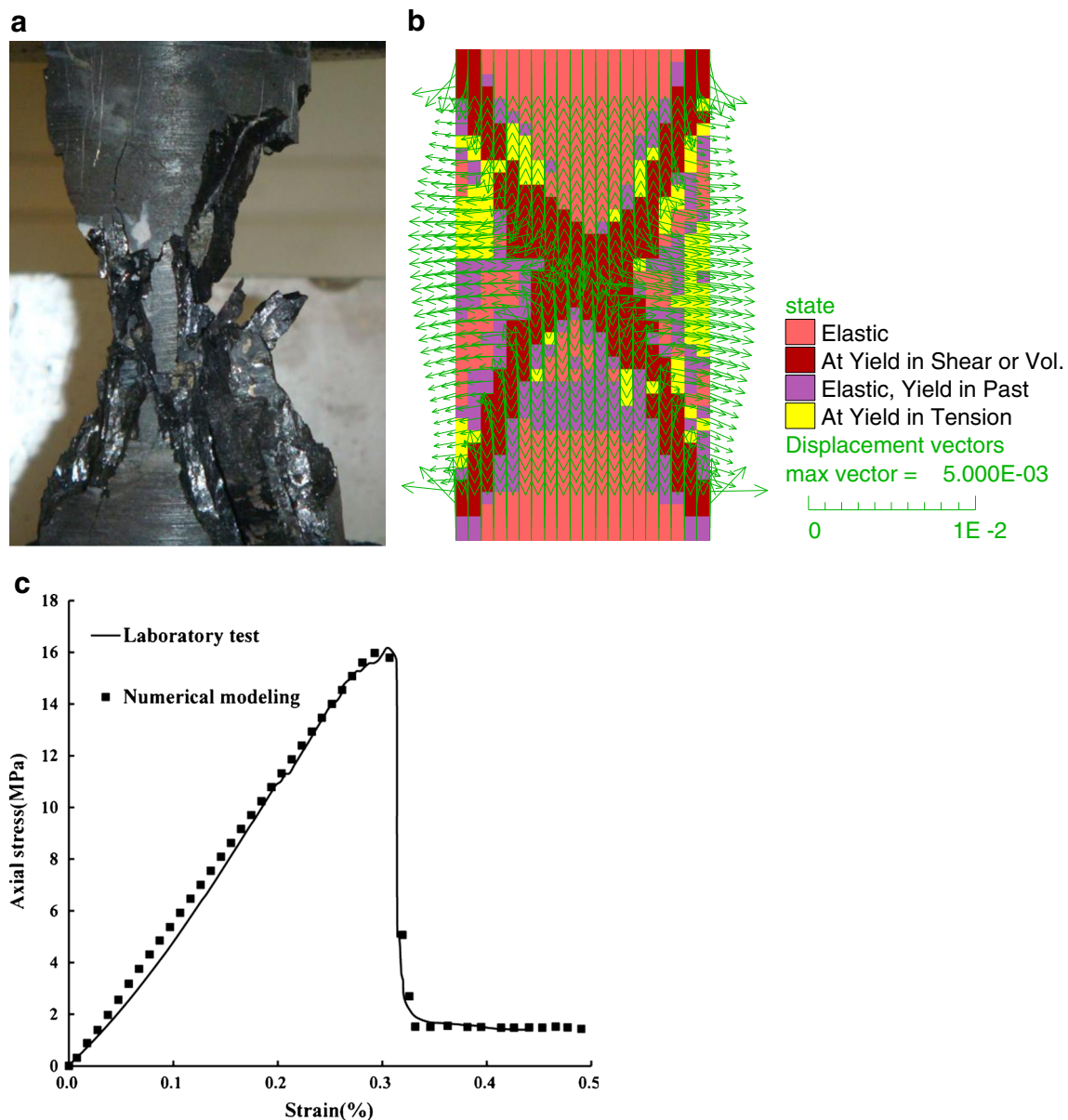


**Fig. 4** Failure patterns and stress–strain curves of laboratory test and numerical simulation on coal uniaxial compression. **a** Failure pattern of the specimen in laboratory test; **b** distribution of plastic zones in numerical model; **c** stress–strain curves



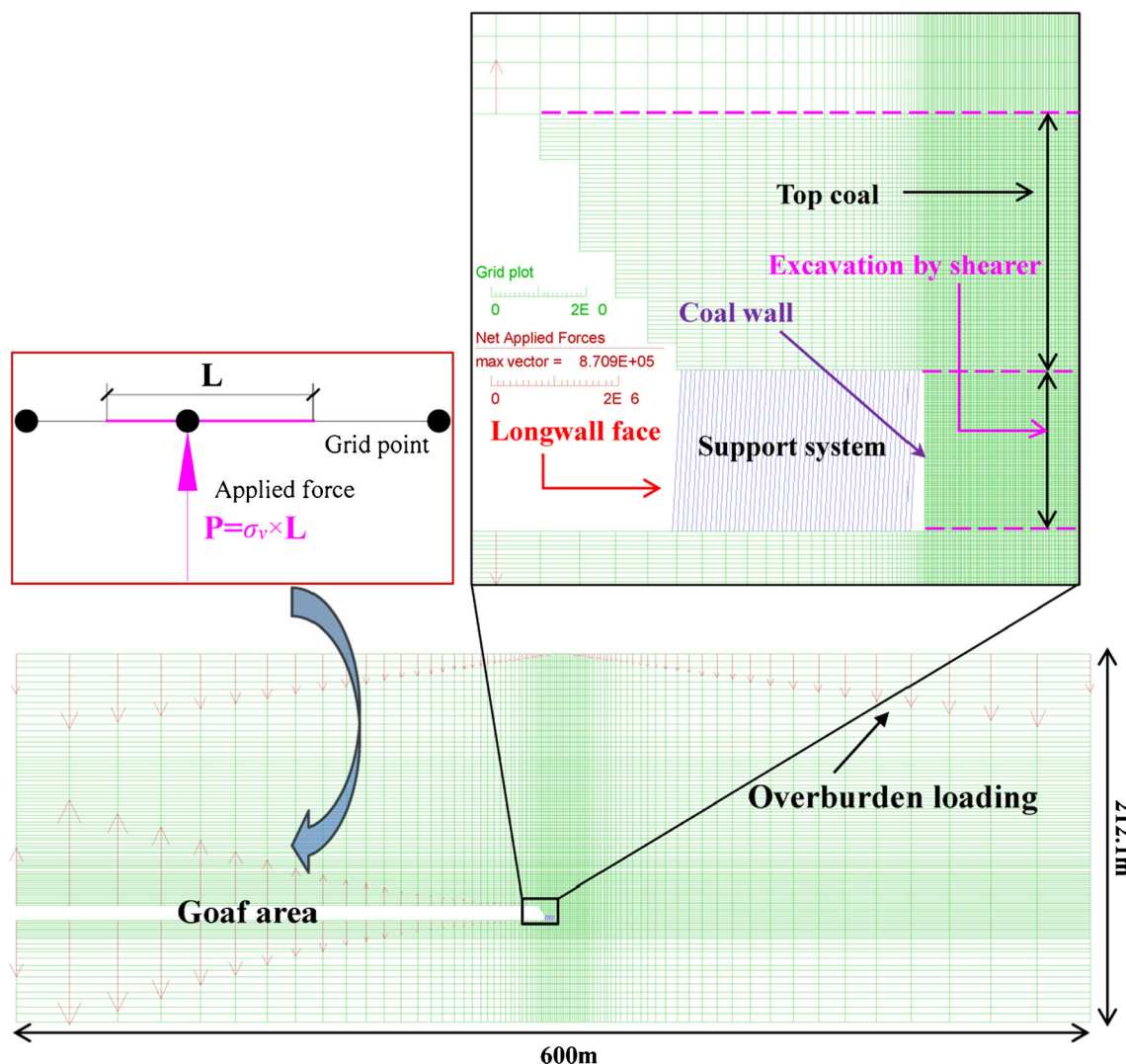


Fig. 5 Finite difference model showing general model layout and boundary conditions

9.1 m. The average depth of #4 coal seam is 574 m. Since the model does not extend to the ground surface, vertical load of 10.74 MPa is applied to the model top to simulate the overburden up to the ground surface. Hypothetically, the initial horizontal stress is equal to the vertical stress. The rock mass in the roof and floor strata is modeled as a Mohr–Coulomb material, while the coal seam is modeled as a strain-softening material, using the built-in constitutive model available in the finite

difference software. A summary of the material properties used in this model is presented in Tables 1 and 2. Due to computation time consumption and capacity restrictions, elements are fined in the face area with the size of 2.5 cm, and magnified gradually along the distance from the face area, as shown in Fig. 5. In total, the model is composed of 50,920 elements and 51,408 grid points. The support elements in the software are used to simulate the shield support in the longwall face.

Table 1 Mechanical parameters of the roof and floor rock masses

Rock mass	$\gamma$ (kg/m <sup>3</sup> )	$K$ (GPa)	$G$ (GPa)	$c$ (MPa)	$\varphi$ (deg.)	$\sigma_t$ (MPa)
Mudstone	2,410	3.28	2.51	5.5	29	2.68
Gritstone	2,550	4.88	2.81	9.5	35.5	3.17
Packsand	2,600	4.88	3.2	9.5	45.5	4.2
Siltstone	2,650	4.18	2.51	7.5	31	3.48
Sandstone	2,500	3.88	2.21	6.5	38	3.08

$\gamma$  is the unit weight,  $K$  is the bulk modulus,  $G$  the shear modulus,  $c$  the cohesion,  $\varphi$  the internal friction, and  $\sigma_t$  the tensile strength

**Table 2** Mechanical parameters of the coal seam

$\gamma$ (kg/m <sup>3</sup> )	$K$ (GPa)	$G$ (GPa)	$C$ (MPa)	$\varphi$ (deg.)	$\sigma_t$ (MPa)	$C_r$ (MPa)	$\varphi_r$ (MPa)	$e_p$
1420	2.58	2.42	3.51	33	2.48	1.58	25	0.05

$C_r$  the residual cohesion,  $\varphi_r$  the residual friction and  $e_p$  the plastic strain parameter at the residual strength

### Longwall goaf simulation

The goaf compaction process is an inseparable part of the longwall mining process since it can change the surrounding loads by acting as an additional support for the system. After extraction of the coal seam, the immediate roof of the mined area caved and compacted behind the working face, causing the stress redistribution around the longwall face. In order to obtain proper induced abutment stress, the goaf compaction process has to be considered when simulating longwall mining. The grid forces are applied on the roof above the goaf area and floor below the goaf area to simulate the support effect supplied by the caved immediate roof (Fig. 5).

The magnitude of the grid force is calculated based on the roof convergence induced at the grid point using Salamon's model (Salamon 1990). In the Salamon's model, the roof convergence is limited at 50 % of the excavated height. The vertical stress generated by the goaf material at this convergence is equal to the virgin vertical stress. As the goaf consolidates gradually, the stress in the goaf increases consequently. The following equation (Badr 2002) is used to describe the stress–strain behavior of goaf material

$$\sigma_v = \frac{E_0 \varepsilon_v}{1 - \varepsilon_v / \varepsilon_m} \quad (1)$$

where  $\sigma_v$  is the vertical stress applied to the goaf material,  $\varepsilon_v$  is the current vertical strain under the applied stress,  $E_0$  is the initial secant deformation modulus, and  $\varepsilon_m$  is the maximum possible strain of the caved rock material.  $\varepsilon_m$  and  $E_0$  are two essential parameters to describe the complete stress–strain curve for a site-specific caved rock material.  $\varepsilon_m$  merely depends on the bulking factor of caved immediate roofs,  $d$ , and it can be determined as follows (Saeedi et al. 2010)

$$\varepsilon_m = \frac{d-1}{d} \quad (2)$$

Equation (1) could be rewritten by Badr (2002)

$$\sigma_v = \frac{a \times \varepsilon_v}{b - \varepsilon_v} \quad (3)$$

where  $a$  is a constant that determines goaf's deformation modulus and  $b$  is the maximum vertical strain.  $a$  and  $b$  are

empirically derived parameters, which can be determined by model calibration and laboratory test.

It was found that strong sandstone goaf material had a stiffer response than the weak shale material, as expected. Goaf filled with strong rock types is less compressible than that filled with weak rock types, that is, the goaf compaction characteristics directly depend on rock type above the coal seam. To assist in selecting the appropriate goaf parameters, a series of  $a$  and  $b$  in Eq. (3) were given by Esterhuizen et al. (2010), who accounted for the type of overburden rock characteristics, as shown in Table 3. In Table 3, weak rocks represent the rocks that have a uniaxial compressive strength (UCS) of less than 20 MPa, such as shales and clay stones. Meanwhile, limestone, sandstones, and siltstones with UCS strength above 40 MPa are classified as strong rocks.

The compaction loads are represented as upward and downward forces that are applied at the grid points of the goaf roof and floor behind the longwall face. After the coal seam has been excavated, vertical displacements at goaf roof grid points are restored and then divided by the seam height to calculate the vertical strain  $\varepsilon_v$  at each grid point. Equation (3) is used to evaluate the vertical stress  $\sigma_v$  at each grid point. The force  $P$  applied to grid point is calculated by multiplying the vertical stress at the grid point by the influence length  $L$  as shown in Fig. 5.

The developed numerical modeling results are compared to empirical vertical stress changes determined from the model of Wilson (1983) as shown in Fig. 6. The in situ vertical stress which is calculated by gravitational approach is 14.35 MPa. It can be observed that the numerical model predicted a peak abutment stress of 65.45 MPa with a distance of 9.6 m in front of the face. This value is in agreement with that determined from the Wilson's model, which predicts a peak abutment stress of 62.95 MPa with a distance of 10.3 m in front of the

**Table 3** Parameters for modeling various goaf types (Esterhuizen et al. 2010)

Overburden type	Ratio of strong/weak rocks (%)	$a$ parameter (MPa)	$b$ parameter
Weak	25	5.9	0.44
Moderate	35	8.6	0.44
Strong	50	12.8	0.44
Very strong	65	25.2	0.44

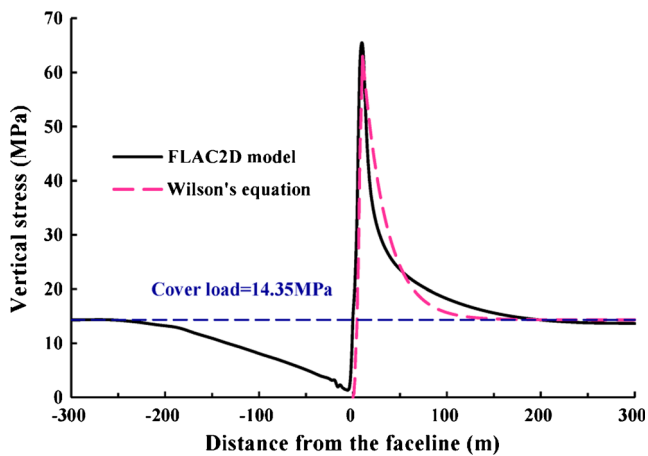


**Fig. 6** Vertical stress redistribution around the longwall face

face. Although the attenuation rate of the FLAC modeled abutment stress is more rapid in the first 50 m and slower in the following 150 m than that predicted by the empirical model, it can be concluded that, in general, the numerical

model satisfactorily predicted the correct behavior. The abutment stress gradually decreases to a value equal to in situ stress at a distance about 200 m in front of the face. In the goaf, the vertical stress returns to its original state at a distance about 240 m behind the face.

Comparison between numerical results and field observations

Figure 7 shows the comparison of the failure mode of the coal wall obtained from the numerical simulation with those from the field observations for type I. From Fig. 7a, it can be found that one shear failure band developed from the down corner and two shear failure bands developed from the upper corner of the longwall face, respectively. The three shear failure bands forms two v-shaped failure zones in the intact coal wall, and the depths of these two failure zones are 0.91 and 1.23 m, respectively. The numerical simulation also successfully predicts the v-shaped coal wall spalling, with depths of 0.83 and 0.74 m, as shown in Fig. 7b, c. The intact coal wall is segmented by shear failure bands, causing block coal wall

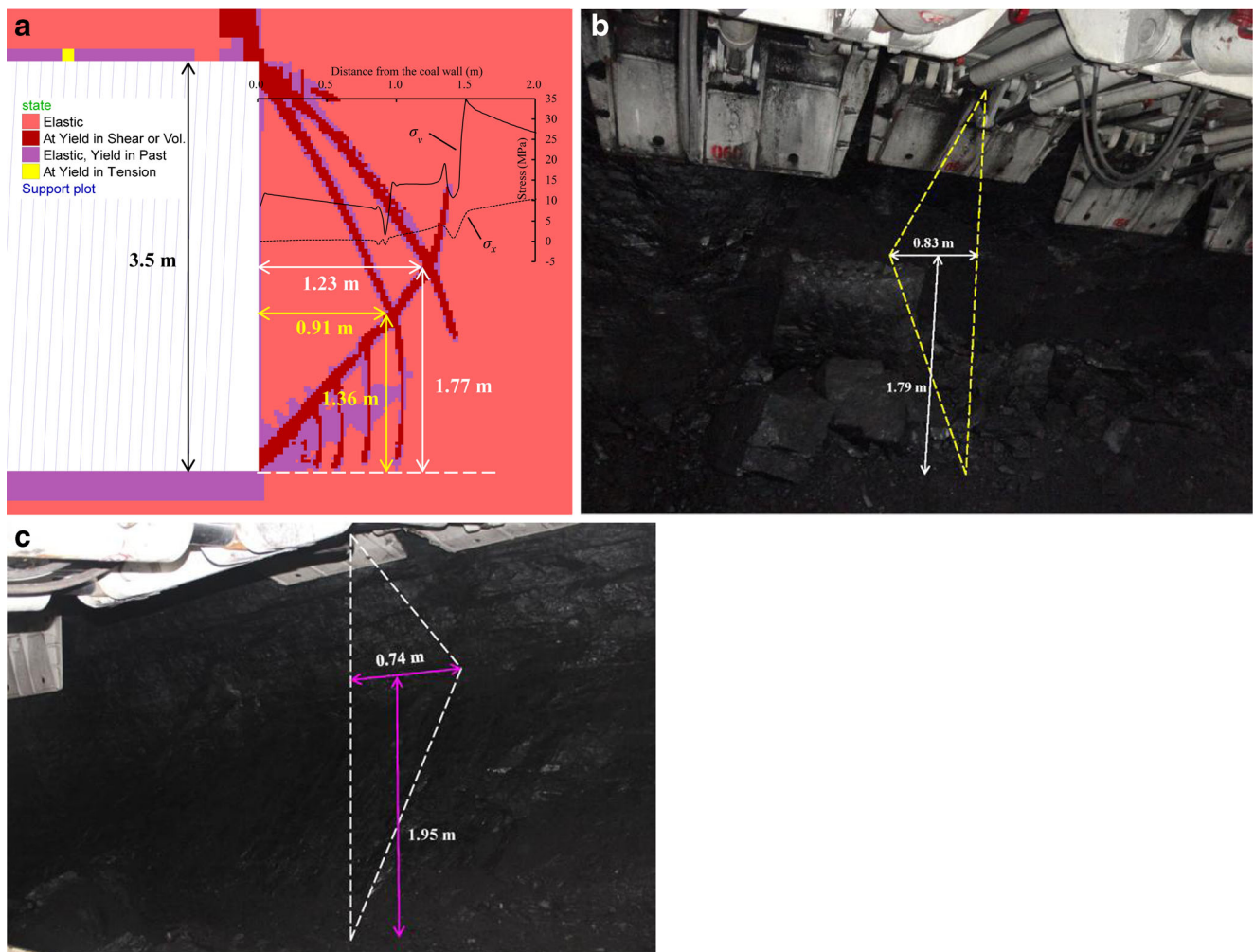


**Fig. 7** Comparison between the numerical results and field observations for type I: **a** numerical results on the intact coal wall, **b** field observation on one site, **c** field observation on another site



spallings, as demonstrated in Fig. 7c. The smooth failure face indicated block spallings slipped from the coal wall. In the lower part of the coal wall, numerical modeling obtains a series of failure bands (see Fig. 7a), and associated small failure zones induce crushed spallings. Another possible reason for small spallings in intact coal wall is that block spallings have a fair chance of crashing into pieces when they slip from coal wall into the chain conveyor. Figure 7a also illustrates the variation of the vertical and horizontal stresses along the face in the middle part of the coal wall. The vertical stress shows a overall rising trend in the first 1.5 m except in the failure areas (shear failure bands) where a stress drop occurs following by a large stress raising. The peak vertical stress is 35 MPa with a distance of 1.5 m from the coal wall, and then gradually declines. The vertical stress in the first v-shaped failure zone is smaller than 10 MPa, indicating that coal mass in this area has failed. It appears a strong possibility that the v-shaped failure zone could spall from the coal wall, because the restrictive horizontal stress in this area is almost zero (Fig. 7a).

Figure 8 shows the comparison of the failure mode of the coal wall obtained from the numerical simulation with those from the field observations for type II (coal wall with a series of 0.15 m space vertical discontinuities). The numerical

results (see Fig. 8a) show that the failure zones mainly develops along the discontinuities except two shear failure bands expanding from the corners of longwall face. Although the vertical discontinuities extend along the whole height of the coal seam (Fig. 3b), few failure zones are found in the top coal. However, discontinuities ahead of the longwall face damage more easily. In the numerical simulation, the depth of the failure is 0.45 m in the upper part and 0.75 m in the lower part of the coal wall. These are very close to those from observed results of field practice, with the depth of 0.43 m in the upper part and 0.68 m in the lower part (see Fig. 8b). Due to the small space of the vertical discontinuities, the major spallings are small fragments. But when the discontinuities have higher strength or the coal wall contains fewer weak discontinuities, block spallings would occur, as show in Fig. 8b. A block spalling with the size of  $1.87 \times 1.52 \times 0.65$  m is formed (viewed from the left hand side of the rectangular area of the dotted line). The horizontal stress at the middle of the coal wall is zero, and shows linear increase with the distance away from the coal wall, as shown in Fig. 8a. The vertical stress along the face increases gradually from 10 to 18 MPa, but large stress drops occur at the first two vertical discontinuities areas while small drops are observed at the later vertical discontinuities. These stress drops suggest that

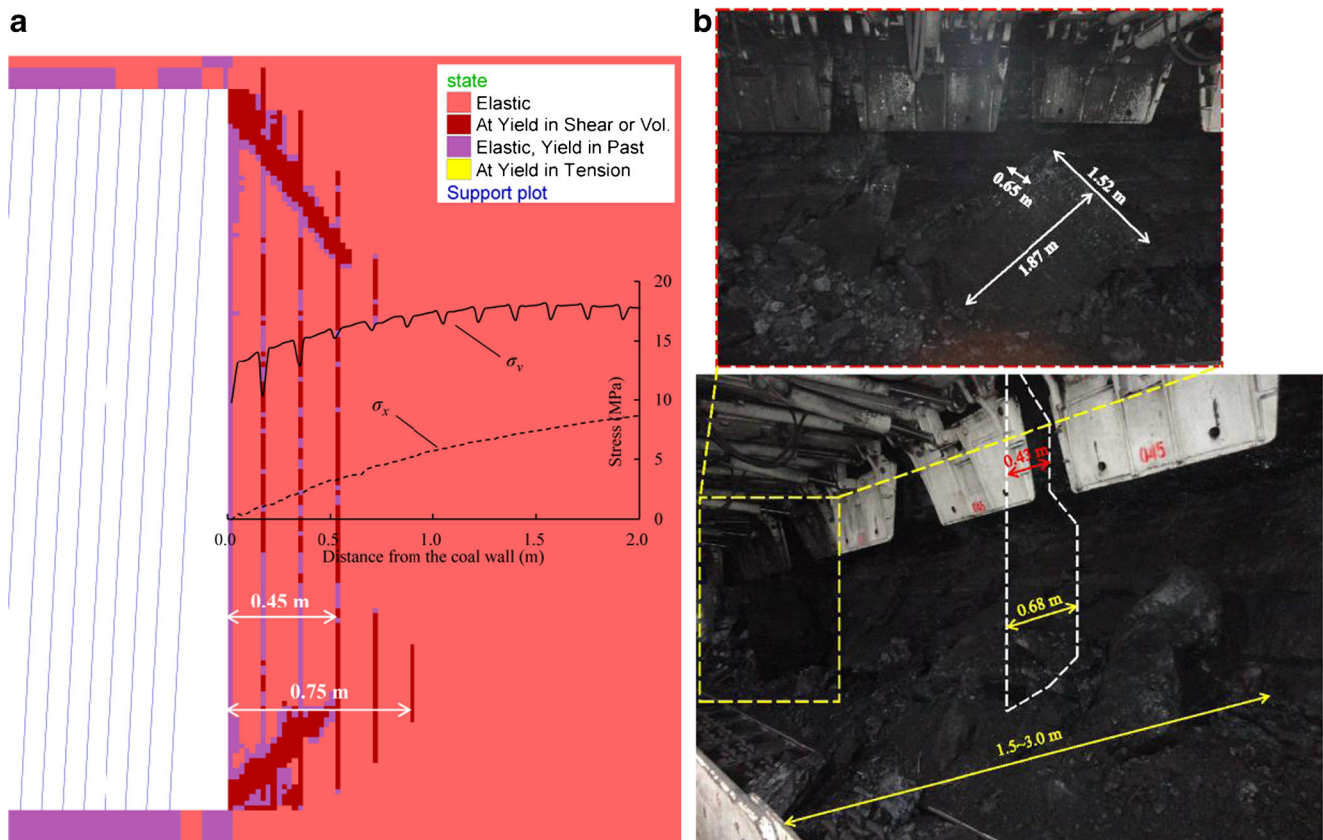


**Fig. 8** Comparison between the numerical results and field observations for type II: **a** numerical results on the coal wall with vertical discontinuities, **b** field observation



the vertical discontinuities are prior to the failure surface, especially for the first several vertical discontinuities where restrictive horizontal stress is relatively small.

Figure 9 depicts the comparison of the failure mode of the coal wall obtained from the numerical simulation with those from the field practice for type III. Similar to the failure mode in type II, besides that the two shear failure zones develop from the corners of the face, the failure zones extend along the criss-cross discontinuities. The numerical result predicts a failure depth of 0.6 m, as shown in Fig. 9a. This value is very

close to those measured at the face, i.e., depth of 0.68 m in the bottom part and 0.35 m in the upper part of the coal seam. Since the coal wall is cut by criss-cross discontinuities, the spallings constitutes of considerable small fragments, as shown in Fig. 9b. The variation of the vertical and horizontal stresses along the face in the model for type III (Fig. 9a) is nearly identical to those in the model for type II. It should be noted that the accessorial horizontal discontinuities make the coal wall more fragmented for type III. The failure depth of the coal wall increases compared to that for type II, but the

**Fig. 9** Comparison between the numerical results and field observations for type III: **a** numerical results on the coal wall with criss-cross discontinuities, **b** field observation

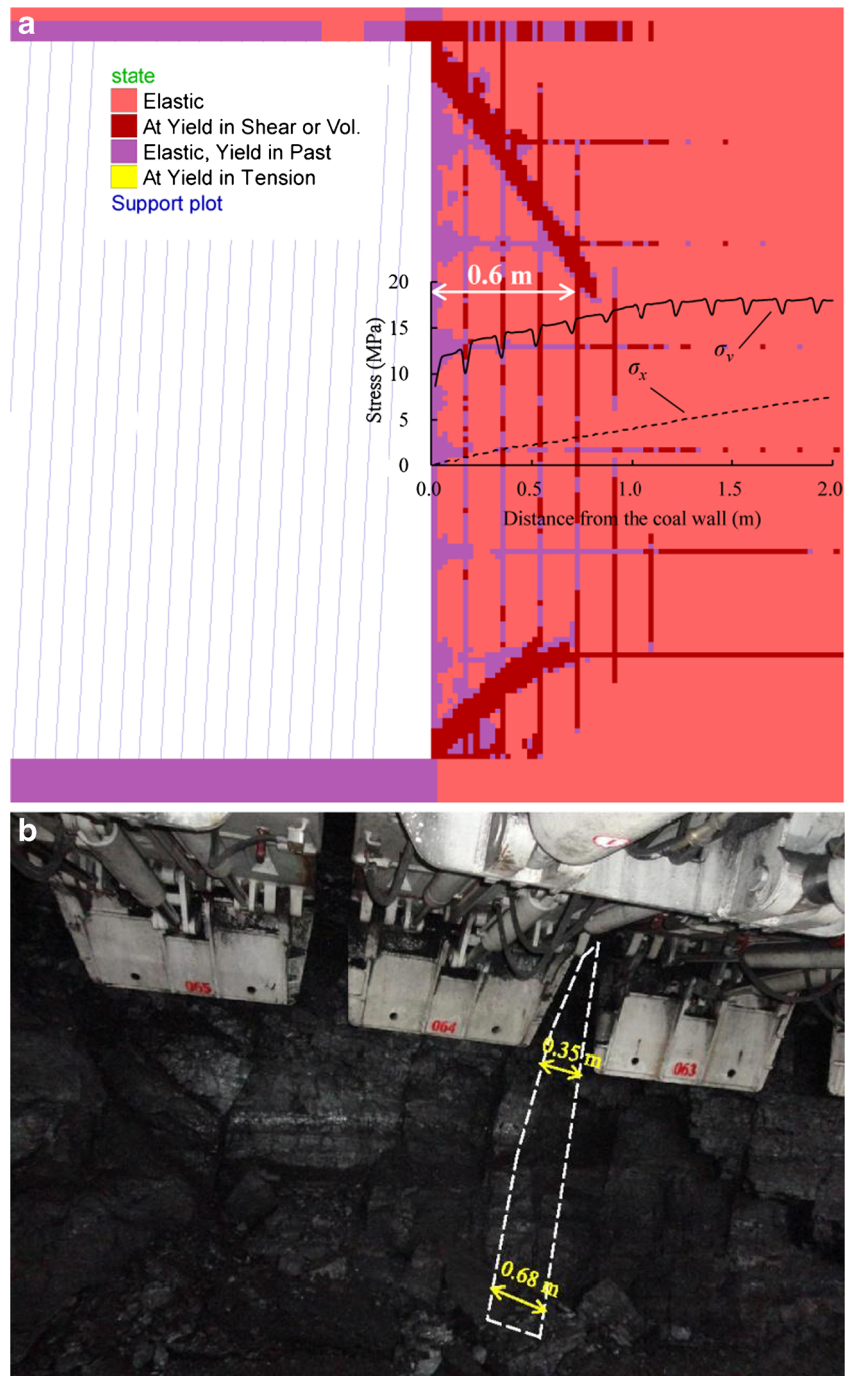


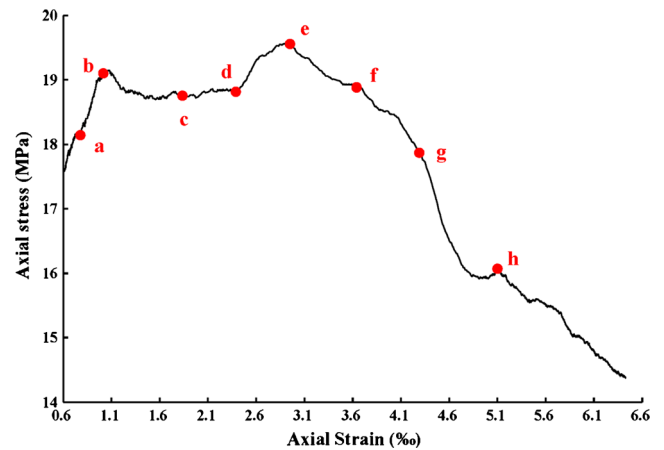
**Table 4** Comparison results between numerical simulations and field observations

Coal wall type	Depth of coal wall spalling (m)		Difference between modeling and measurement	
	Field observation	Numerical simulation	m	%
I	0.79	0.91	0.12	13.2
II	0.56	0.60	0.04	6.7
III	0.52	0.60	0.08	13.3

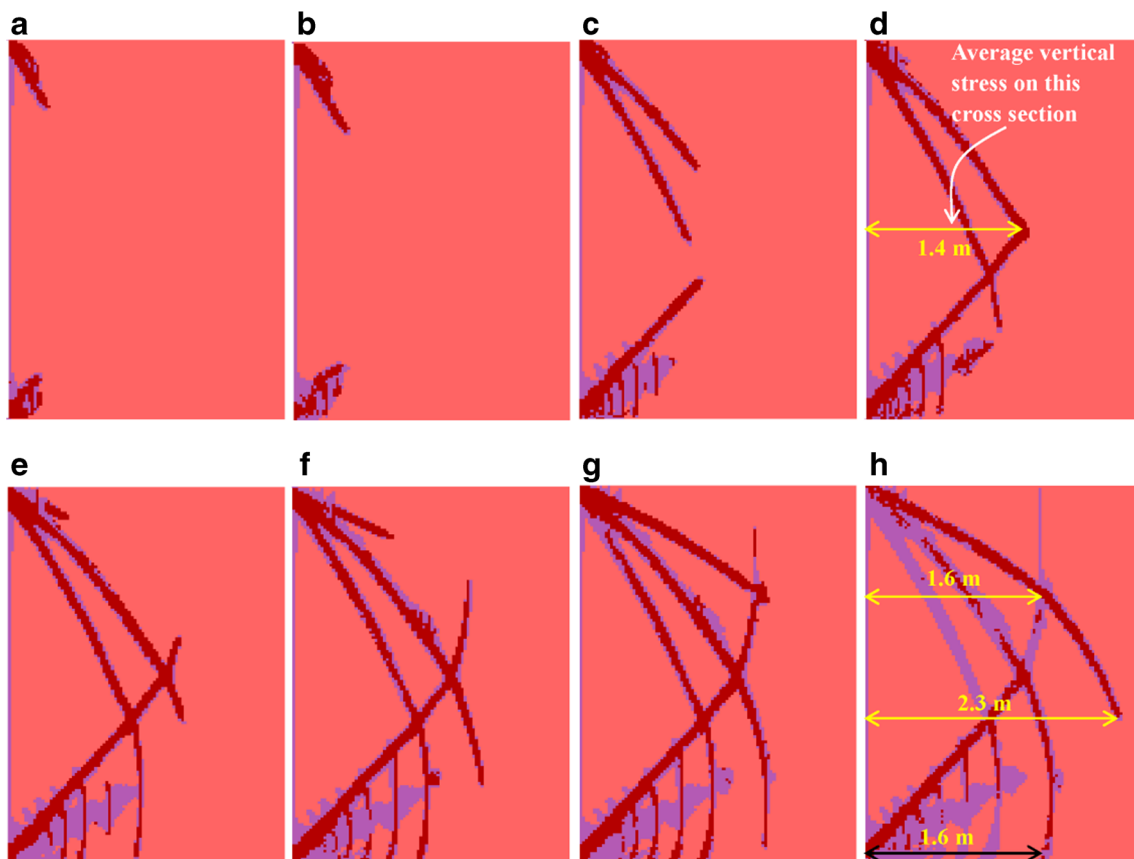
The field observation results in the table are average values

operation of the shearer and chain conveyor is not affected by the crushing spillings.

The comparison of coal wall spalling depth between numerical simulations and field observations are given in Table 4. It can be found that the depth of the coal wall spalling determined by numerical simulations is approximately 10 % greater than that from the field observations. The value of spalling depth in type I (i.e., intact coal wall) is larger than those in the other two types (i.e., coal wall including discontinuities). The main reason is that, at the time of observation, longwall mining is interrupted by machinery maintenance,

**Fig. 11** Axial stress–axial strain relation for the first 1.4 m width of coal wall

and the face waits for a quite long time, resulting in the development of fractures to the deeper part due to increased roof pressure (Bilim and Özkan 2008). This mechanism will be further analyzed in the next section. Despite that the numerical models do not simulate the overall complexity of the longwall face (i.e., discontinuities, strength variations of the coal seam, and roof and floor rock mass), it is considered that the numerical results are credible.

**Fig. 10** Failure processes of intact coal wall

**Discussions**

Field observations found that the pressure applied on the coal wall increased and the coal wall strength degenerated when production stopped, and the fractures in the coal wall extended to deeper part (Bilim and Özkan 2008). In China, when the shearer cutting height is larger than 3.0 m, the tendency of coal wall failure and spallings increase significantly, which results in unexpected accidents including equipment damage and casualties from time to time. Therefore, most shield supports are equipped with face guard (Fig. 1) when the shearer cutting height is more than 3.0 m. In this section, analyses are conducted to study the effects of the face stoppage time and face guard on the failure mode and spallings of the coal wall.

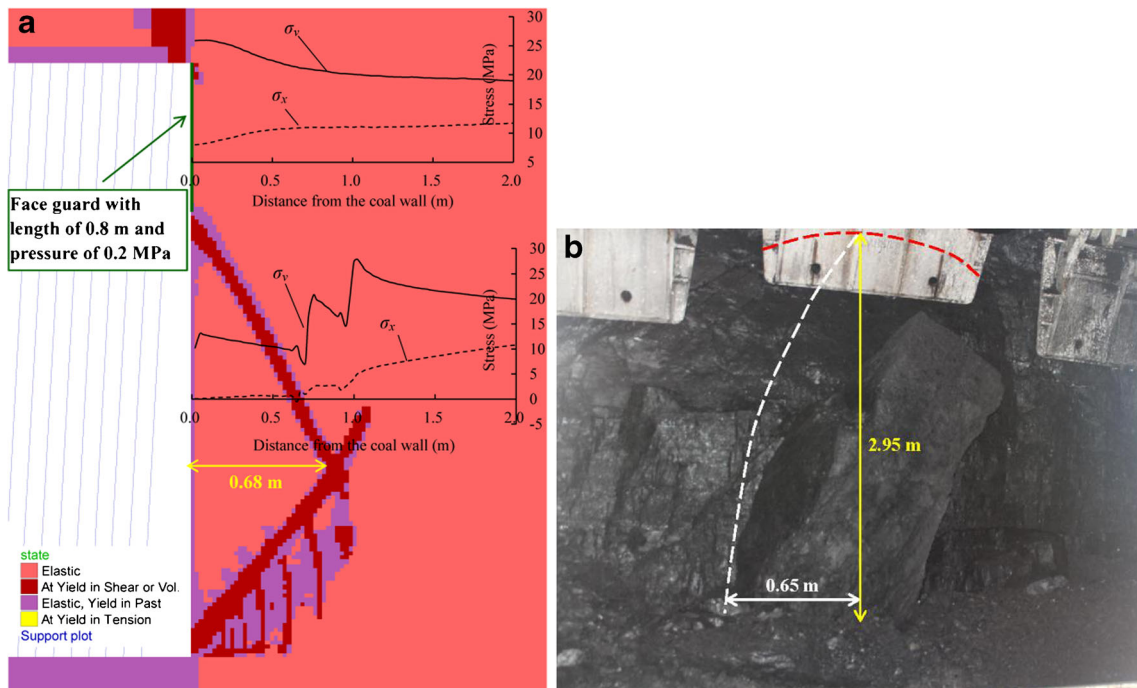
**Influence of the face stoppage time**

Figure 10 shows the coal wall failure development at different stages. Figure 11 shows the average axial stress–axial strain relation for the first 1.4 m width middle coal wall (as defined in Fig. 10d). In the first two stages (i.e., stages a and b), the applied vertical stress on the first 1.4 m width coal wall increase rapidly as the step time increases. In the next three stages (i.e., stages c, d, and e), the vertical stress in the coal wall increases continuously with slightly fluctuations. The failure depth of the coal wall is 1.4 m at this moment, as shown in Fig. 10d. Afterwards, the third shear failure band grows from the upper corner of the face coal (Fig. 10e) and develops to the deeper part (Fig. 10e–h), which corresponds to the stress drops shown in Fig. 11 (stages e–h). At this moment,

the failure depth of the coal wall is 1.6 m in the upper and bottom part and 2.3 m in the middle part (Fig. 10h). After a few further time steps, the vertical stress decreases linearly, and the coal wall becomes unstable. Through the discussion above, it can be seen that coal wall spallings could be avoided if the next mining cycle was carried out before the three shear failure bands (see Fig. 10c) intersects. Therefore, in field practice, the coal wall spallings may be relieved though accelerating the mining operation and reduction of face stoppage time.

**Influence of the face guard**

In 14101 longwall face, each shield support is equipped with a face guard with a length of 0.8 m and maximum pressure of 0.2 MPa that is applied to the coal wall. Figure 12 illustrates the failure and spalling mode for intact coal wall protected by the face guard. It can be seen that the upper part of coal wall has no damage under the protection of face guard, and a shear failure band develops from the end point of the face guard, as shown in Fig. 12a. Comparing with coal wall without face guard protection (Fig. 7a), the depth of the failure zone decreases from 0.91 to 0.68 m. Field practice also show the same spalling mode, as can be seen in Fig. 12b. The height of the spalling is 2.95 m, rather than the whole height of the face; the failure plane is cambered with a maximum depth of 0.65 m. These values are consistent with the numerical results. The stress distribution along the face at the bottom part (unprotected area) of the coal wall is similar to those without face guard protection (Fig. 7a). While at the face guard area, the



**Fig. 12** Coal wall failure mode and spalling for intact coal wall under protection of face guard: **a** numerical result, **b** field observation

peak vertical stress is large (26 MPa) but decreases to 19 MPa. The horizontal stress is 8 MPa, and gradually increases to 12 MPa, as shown in Fig. 12a. The large stress suggests that the coal wall remain stable in the protective area.

Figure 13 shows the failure and spalling mode for vertical discontinuities coal wall protected by the face guard. The failure depth is 0.45 m in the middle part of the coal wall and increases to 0.60 m in the lower part. But the upper part remains intact under the protection of the face guard, as shown in Fig. 13a. Field practice also shows that when the face guard is opened in time (i.e., just after the shearer passes), the upper part of the coal wall could maintain stable, as shown in Fig. 13c, d. From Fig. 13b, a block face spalling with a height of 2.65 m and depth of about 0.56 m is observed. Figure 13c

presents relative small segment spillings with a height of 2.93 m and depth of 0.38 m, i.e., the spillings take place mainly in the middle and bottom part of the coal wall. This is crucial to the safety of workers and equipments because the maximum width of the shearer corridor is 3.0 m (see Fig. 8b), some fragments could fly into the worker walk tunnel in the shield support when block coal (with a height of more than 3.0 m) falls down from the face and crushes, which could lead to unexpected accidents. Figure 13a also exhibits the variation of the vertical and horizontal stresses in the upper and bottom area. The stress distribution along the face at the bottom part (unprotected area) of the coal wall is inconsistent with those without face guard protection (Fig. 8a). While at the protected area, the stress distribution characteristics are similar to those

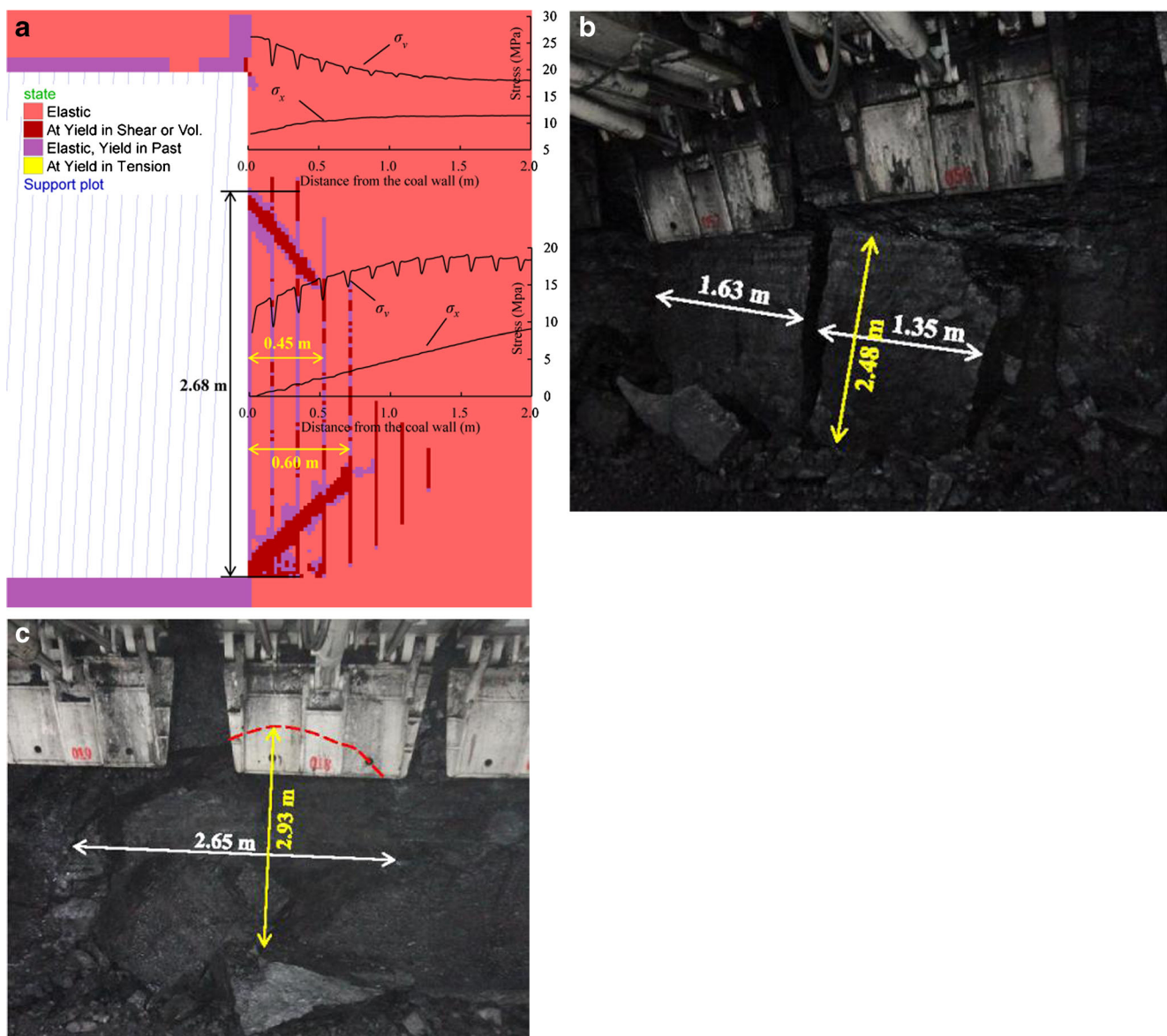


**Fig. 13** Coal wall failure mode and spillings for vertical discontinuities coal wall under protection of face guard: **a** numerical result, **b** field observation on one site, **c** field observation on another site



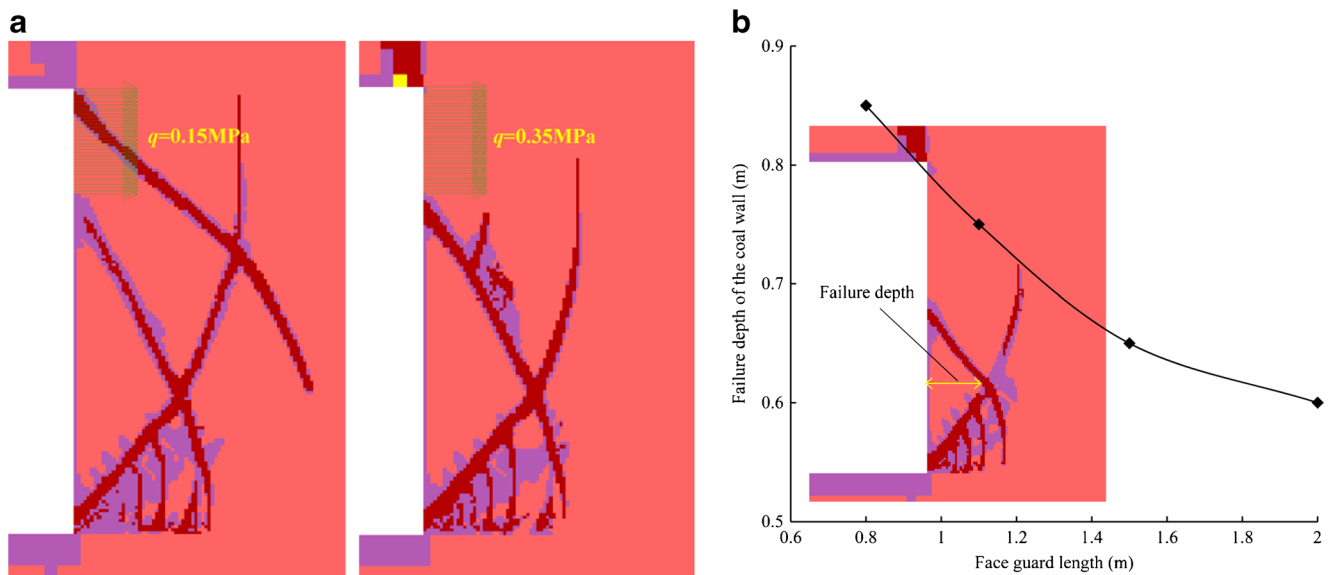


**Fig. 14** Coal wall failure by the influence of face guard pressures and lengths: **a** coal wall failure modes with the influence of different face guard pressures; **b** failure depths of the coal wall with the influence of different face guard lengths

of intact coal wall protected by the face guard (Fig. 12a), except for that the vertical stress presents several small drops at the discontinuities. But the small stress drops have relatively low negative impact on the stability of the coal wall.

Numerical simulations also show that the upper part of the coal wall cannot remain stable when the protecting pressure supplied by the face guard is smaller than 0.2 MPa. When the protecting pressure is 0.15 MPa, there is a shear failure band developing from the upper corner. Once it meets another shear band developing from the down corner, a potential spallings in the upper part of the coal wall could be formed. However, when the protecting pressure increases to 0.35 MPa, no failure zones appear in the upper part of the coal wall, as shown in Fig. 14a. As can be seen, when the face guard pressure is greater than 0.2 MPa, the protected area is able to remain stable and the failure height of the coal wall decreases accordingly. Consequently, the failure depth in the unprotected area reduces, as shown in Fig. 14b. When the face guard length increases from 0.8 to 2.0 m, the failure depth decreases from 0.85 to 0.6 m. From the numerical results and field practices, it is shown that under the circumstances of 14101 longwall face, the length of the face guard is not large enough, and the protecting pressure applied to the coal wall tends to be small.

## Conclusions

In this study, a 2D model is constructed for the purpose of examining the brittle failure of coal wall during longwall mining in Majialiang coal mine. The strain-softening constitutive model is used to analyze the brittle failure characteristics

of the coal wall. A numerical algorithm is developed to simulate the longwall goaf compaction process, and obtain the proper mining induced stress around the longwall face. The numerical results of coal wall failure modes and spalling depths are consistent with the field observations.

Both the field observations and the numerical results show that the coal wall presents a brittle failure mode, which always forms block spallings in the longwall face, threatening the safety of the workmen and equipments in the work space. The failure mode and failure depth (from numerical results) or spalling depth (from field observation) of the coal wall is dominated by the shear failure bands that develop from the down and upper corners of the longwall face. For the intact coal wall case, the failure mode presents v-shaped failure zones, and the failure (spalling) depth ranges 0.7–0.8 m. Block coal wall spallings are favorable to be formed, which has negative impact on safety and mining operation. For the case of coal wall including vertical discontinuities, small space vertical discontinuities causes small fragment spallings with depth of 0.4–0.7 m, while large space vertical discontinuities leads to relatively larger block spallings. For the case of coal wall including criss-cross discontinuities, the failure depth is about 0.6 m and the spallings are constituted of considerable small fragments, which probably do not disturb the mining process.

Face stoppage time has a significant influence on the failure depth of the coal wall. As the stoppage time increases, the vertical pressure applied on the coal wall increases and the strength of the coal wall weakens (Bilim and Özkan 2008), leading to the shear failure bands in the coal wall developing to the deeper part. Coal wall spallings could be avoided if the next mining cycle is implemented before the shear failure

bands connect. In the field practice, the mining operation should accelerate to reduce the face stoppage time and relieve the induced stress applied on the coal wall, such that coal wall strength weakens could avoid. The results also shown that the face guard equipped on the shield support is able to protect the upper part of the coal wall from failing and spalling. The spallings height and depth decrease, correspondingly, to a certain degree, reducing the probability of formation of large block spallings.

From the numerical results and field practices, it is also suggested that the length of the face guard should be enlarged and the protecting pressure should be increased in 14101 longwall face. The proposed numerical approach in this paper successfully demonstrates stability analysis of coal wall in longwall face, and can serve as a guide to the design of the face guard equipped on the shield support.

**Acknowledgments** Financial support for this work is provided by the Priority Academic Program Development of Jiangsu Higher Education Institutions (SZBF2011-6-B35), the Graduate Students of Jiangsu Province Innovation Program (CXZZ13\_0948), and Research Found for the Doctoral Program of Higher Education of China (20120095120017).

## References

- Badr SA (2002) Numerical analysis of coal yield pillars. Ph.D. thesis. Mining Engineering Department, Colorado School of Mine, p 188
- Bai QS, Tu SH, Wang FT, Yuan Y (2012) Stress evolution and induced accidents mechanism in shallow coal seam in proximity underlying the room mining residual pillars. *Chin J Rock Mech Eng (Suppl. 2)*: 3772–3778 (in Chinese)
- Bai QS, Tu SH, Wang FT, Zhang XG, Tu HS, Yuan Y (2013) Observation and numerical analysis of the scope of fractured zones around gateroads under longwall influence. *Rock Mech Rock Eng*. doi:10.1007/s00603-013-0457-9
- Bilim N, Özkan İ (2008) Determination of the effect of roof pressure on coal hardness and excavation productivity: an example from a Çayırhan lignite mine, Ankara, Central Turkey. *Int J Coal Geol* 75: 113–118
- Edelbro C (2010) Different approaches for simulating brittle failure in two hard rock mass cases: a parametric study. *Rock Mech Rock Eng* 43(2):151–165
- Esterhuizen E, Mark C, Murphy MM (2010) Numerical model calibration for simulating coal pillars, gob and overburden response. In: *Proceedings of the 29th International Conference on Ground Control in Mining*, West Virginia, pp 44–57
- Ju JF, Xu JL (2013) Structural characteristics of key strata and strata behavior of a fully mechanized longwall face with 7.0 m height chocks. *Int J Rock Mech Min Sci* 58:46–54
- Liu ZL, Zhang ZW (2010) Analysis for “8.24” roof fall accidents of Muchengjian mine. *Coal Eng* 90:49–51 (in Chinese)
- Liu CY, Huang BX, Chang XM, Wang J, Wei MT (2008) Study on tip-to-face coal and rock stability control of fully mechanized stepped large cutting height mining in extremely soft thick seam. *J China Univ Mini Technol* 37(6):734–739 (in Chinese)
- Mortazavi A, Hassani FP, Shabani M (2009) A numerical investigation of rock pillar failure mechanism in underground openings. *Comput Geotech* 36(5):691–697
- Ning Y (2009) Mechanism and control technique of the rib spalling in fully mechanized mining face with great mining height. *J China Coal Soc* 34(1):50–52, 9 (in Chinese)
- Pappas DM, Bauer ER, Mark C (2000) Roof and rib fall incidents and statistics: a recent profile. In: *Proceedings: new technology for coal mine*. Pittsburgh, USA, p 3–21
- Saeedi G, Shahriar K, Rezaei B, Karpuz C (2010) Numerical modelling of out-of-seam dilution in longwall retreat mining. *Int J Rock Mech Min Sci* 47:533–543
- Salamon M (1990) Mechanism of caving in longwall coal mining. In: *Proceedings of the 31st US rock mechanical symposium*. Golden, p 161–168
- Schullera H, Schweiger HF (2002) Application of a multilaminar model to simulation of shear band formation in NATM-tunnelling. *Comput Geotech* 29(7):501–524
- Wang JC (2007) Mechanism of the rib spalling and the controlling in the very soft coal seam. *J China Coal Soc* 32(8):785–788 (in Chinese)
- Wang SY, Sloan SW, Huang ML, Tang CA (2011a) Numerical study of failure mechanism of serial and parallel rock pillars. *Rock Mech Rock Eng* 44:179–198
- Wang SL, Zheng H, Li CG, Ge XR (2011b) A finite element implementation of strain-softening rock mass. *Int J Rock Mech Min Sci* 48:67–76
- Wilson AH (1983) The stability of underground workings in the soft rocks of the coal measures. *Int J Min Eng* 1:91–187
- Yuan Y, Tu SH, Wu Q, Ma XT, Tu HS, Sun LL (2011) Mechanics of rib spalling of high coal walls under fully-mechanized mining. *Min Sci Technol (China)* 21(1):129–133
- Yuan Y, Tu SH, Ma XT, Sun LL, Bai QS (2012) Coal wall stability of fully mechanized working face with great mining height in “three soft” coal seam and its control technology. *J Min Saf Eng* 29(1):21–25 (in Chinese)
- Zhang Q, Jiang BS, Wang SL, Ge XR, Zhang HQ (2012) Elasto-plastic analysis of a circular opening in strain-softening rock mass. *Int J Rock Mech Min Sci* 50:38–46
- Zhou JW, Xu WY, Li MW, Zhou XQ, Shi C (2009) Application of rock strain softening model to numerical analysis of deep tunnel. *Chin J Rock Mech Eng* 28(6):1116–1127 (in Chinese)
- Zhu T (2010) Study on the surrounding rock control theory and technology of soft seam in high mining height longwall face. Ph.D. thesis. College of Mining Technology, Taiyuan University of Technology (in Chinese)